



## UNCERTAINTY AND SENSITIVITY ANALYSES OF SOURCE TERM ESTIMATES DURING AN UNMITIGATED SBO SEQUENCE IN A PWR-1000 REACTOR

Autor **Rafael Iglesias**, **Michela Angelucci**<sup>2\*</sup>, **Sandro Paci**<sup>2</sup>, **Luis E. Herranz**<sup>1</sup>

<sup>1</sup> Centro de Investigaciones Energéticas y Medioambientales (CIEMAT), Avda. Complutense, 40, 28040, Madrid, España.

<sup>2</sup> Universitat di Pisa (UNIFI), Iargo Lucio Lazzarino, 56122, Pisa, Italy.

[\\*rafael.iglesias@ciemat.es](mailto:rafael.iglesias@ciemat.es), [\\*michela.angelucci@ing.unipi.it](mailto:michela.angelucci@ing.unipi.it)

### Summary

The Management and Uncertainties of Severe Accidents (MUSA) project is focused on the testing, adaptation, and use of Uncertainty Quantification (UQ) and sensitivity methods for the application in Severe Accident (SA) analysis. An Uncertainty and Sensitivity Analysis (UaSA) of source term (ST) estimates in a Best Estimate Plus Uncertainty (BEPU) calculation of an unmitigated Station Black-Out (SBO) occurring in a 3-loop PWR-W has been conducted by CIEMAT in collaboration with University of Pisa. The results of the analysis provided some major insight. The ST magnitude is affected by a small uncertainty band. Sensitivity analysis did not point at any phenomenon of outstanding significance; however, the time of fuel failure and the diffusional release of radionuclide from fuel have been found to affect the ST to the environment.

**KEYWORDS:** SOURCE TERM, SEVERE ACCIDENT, BEPU, SBO, PWR

### 1. INTRODUCTION

The Management and Uncertainties of Severe Accidents (MUSA) project, led by CIEMAT, is focused on the testing, adaptation, and use of Uncertainty Quantification (UQ) and sensitivity methods for the application in Severe Accident (SA) analysis. Within the project, which is structured in different Work Packages (WPs), the application of the above-mentioned methods is proposed, in WP5, for what concerns the evaluation of the Source Term (ST) in selected SA scenarios for different types of Light Water Reactors (LWRs). In this regard, CIEMAT in collaboration with University of Pisa carried out an Uncertainty and Sensitivity Analysis (UaSA) of ST estimates in a Best Estimate Plus Uncertainty (BEPU) calculation of an unmitigated Station Black-Out (SBO) occurring in a 3-loop PWR-W. The objective of this paper is to present the results of the analysis performed.

### 2. SBO SCENARIO. BASE CASE

#### 2.1. Scenario description and main assumptions.

The simulated scenario is an unmitigated Station Black Out (SBO) in a generic nuclear power plant with a Generation II 3-loop Pressurized Water Reactor (PWR) designed by Westinghouse.

It is assumed that the reactor operated at full power before the transient. In the modeling were considered the availability of the accumulators, two turbo-pumps of the auxiliary feed water system (AFW), batteries (duration 6 hours) and the functioning of the safety valves (Steam generators and Pressurizer). The unavailability of the high- and low-pressure injection systems, also was considered.

The analysis of the sequence includes the following failures:

- AFW turbines fail when the Main Steam Lines (MSLs) become flooded.
- MSLs fail when water level reaches half pipe height.
- Hot Leg creep failure (MELCOR model [2]).
- Containment over-pressure ( $P > 8$  bar / Design Pressure  $\sim 3.8$  bar) [3].
- Vessel Failure due the thermal creep

The accident sequence time span is 48 h and not severe accident management actions were considered. The analysis of the accident was focused on the released activity to the environment after containment failure (Source Term).

### **2.1.1. Plant model.**

In Figure 1 is illustrated the plant model implemented in MELCOR 2.2 code [1,2]. The nodalization of the NSSS (Nuclear Steam Supply System) includes the primary and secondary systems. The RCS (Reactor Coolant System) is modelled as 3 loops and it includes components such as pressurizer, RPV (Reactor Pressure Vessel), accumulators, RWST (Refuelling Water Storage Tank), etc.

The RPV is modelled into 10 interconnected control volumes: downcomer, lower plenum, core region (5 control volumes), bypass, upper-plenum and upper head. Compartment connections are modelled as flow paths, some of which are controlled through valves. The RPV core barrel, internals and guide tubes structures are modelled using heat structures.

The core is divided in 6 radial rings and 13 axial nodes for core degradation modelling (COR package). The first five rings represent the fuel, and the sixth ring represents the core bypass region.

The secondary system nodalization includes the steam generators (SGs), the model of the feed water system and the pipelines representing the MSLs. The secondary side of every SG is modelled in two control volumes, one of which is the SG downcomer. Two control volumes represent the ascending and descending SG tubes.

The large dry containment nodalization is represented with 30 control volumes interconnected through flow paths. The input deck contains 94 control volumes (CVH), 178 flow paths (FL) and 326 heat structures (HS).

The MELCOR RN package is used for the modelling of transport and behaviour of the fission products. Thus, radionuclides are modelled in 17 RN classes where CS is class 2, I2 is class 4, CSI is class 16 and CSM is class 17. The temperature for gap release is set up to 1173K, and the used released model is the revised CORSOR-BOOTH for high burn-up.

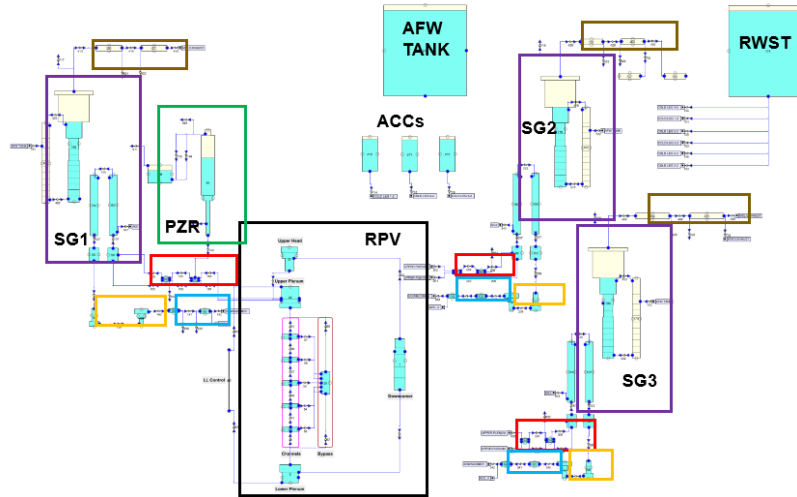


**Figure 1. NPP MELCOR nodalization.**

### 2.1.2. Transient analysis results.

The accident sequence starts with the loss of offsite power and failure of onsite emergency AC (Alternate Current) power (SBO event) followed by the reactor trip and MSIV (Main Stem Isolation Valve) closure. The DC (Direct Current) buses are available for instrumentation, PORV (Power Operated Relief Valve) operation, and Turbine Driven Auxiliary Feed Water (TDAFW) operation.

After the reactor trip and the beginning of the auxiliary feed water system, the primary pressure decreases (Figure 2) until the pressurizer empties at 22.9 h. At this time of the transient, the decay power is still effectively removed from the core. As a result of the closure of MSIVs, the pressure in the SGs increases leading to the opening of the PORV in the SG1. The initial opening of the PORV of the SG1 causes a rapid decrease of the pressure in the other SGs until the depletion of the AFW flow rate to all the SGs at approximately 1.8 h. After this time the pressure in all SGs begins to increase reaching the PORVs set point.

Due to the AFW system injection, the water level in all SGs increases. When the batteries run out, the auxiliary feed water pumps run at full capacity without regulation, leading to the filling of all SGs. The filling of the steam generator comes first in SG1 causing a steam line break (MSLB) in this SG and release of the water material to the containment. As a result of the MSLB, at 7.4 h, the SG1 pressure and level decrease until its complete depressurization (Figure 2) and dry out.

After the MSLB, the pressurizer water level begins to increase and therefore the primary pressure and pressure in the SGs (SG2 and SG3). The pressurizer filling causes the increase of the pressure in the pressurizer relief tank until the reaching of the set point pressure for the relief tank disk failure at approximately 21.0 h.

At approximately 27.3h occurs the creep rupture (modelled according the MELCOR model [2]) in the hot third leg. As result of the rupture, high pressure water is released to containment causing the increase of the containment pressure. After the RPV fail at 30.1 h and corium debris relocation, the containment pressure increases reaching the set point from the containment failure at 39.8 h.

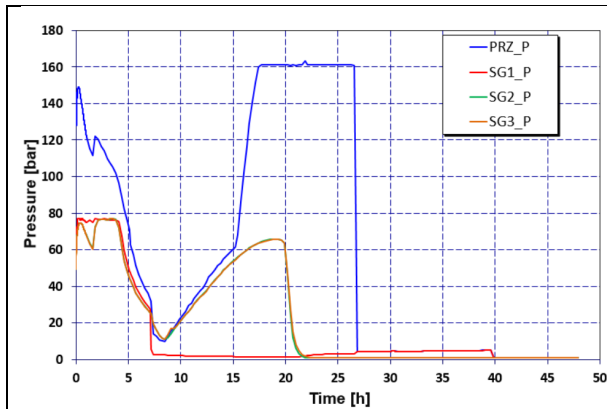


**Figure 2. Evolution of the primary and SG pressure.**

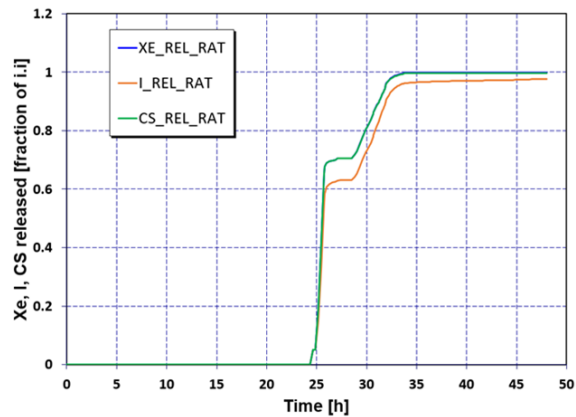


**Figure 3. Release of Xe, I<sub>2</sub>, Cs (fraction of i.i) from the fuel.**

Figure 3 above shows the release of Xe, I<sub>2</sub> and Cs respectively, as a fraction of the i.i. According to the figures 100 % of the Xe and Cs and almost 99.8% of I<sub>2</sub> are released from the core.

The release to environment of radioactive materials begins after the containment failure. At the end of the transient approximately 90% of Xe and 86 % of I<sub>2</sub> are released to the environment. A similar behaviour should be expected for Cs. Regrettably, a mistake was made in the input deck when distributing Cs in different classes in MELCOR and it was unnoticed. This led to an underestimate of Cs release to the environment (30 %i.i). Regardless the quantitative mistake for Cs release to the environment, it was kept for the phase of uncertainty propagation as it was already launched when the BE was analysed. This emphasizes how important is to proceed sequentially and conduct a deep consistency analysis of BE results before getting involved in the next “multiple realizations phase”. Such an analysis should be based on the most grounded engineering judgement available. In the following Table 1 the chronology of events of the SBO simulation is presented.

**Table 1. Timing of the main SBO sequence events.**

| Key Event                                                              | Time    |
|------------------------------------------------------------------------|---------|
| SBO                                                                    | 0.0 s   |
| Reactor SCRAM                                                          | 0.0 s   |
| All RCPs tripped                                                       | < 1.0 s |
| AFW system start                                                       | 10.0 s  |
| MSL 1 break (water discharge into the containment)                     | 7.4 h   |
| Hot leg creep rupture                                                  | 27.3 h  |
| Vessel failure and start of the corium debris relocation in the cavity | 30.1 h  |
| Containment failure and beginning of radioactive release               | 39.8 h  |

### 3. UNCERTAINTY AND SENSITIVITY ANALYSIS

For the Uncertainty Analysis (UA), the MELCOR 2.2 code (version 2.2.21402) has been employed in combination with DAKOTA 6.7 [3] as UQ tool using developed complex Python scripts.

Taking into account the complexity of the SA phenomenology, a huge number of Input Parameters (IPs) might contribute to uncertainties in the Figures Of Merit (FOMs). Thus, a large set of input parameters should be selected to conduct a comprehensive uncertainty analysis, however, the expertise gained in MUSA project analysis highlighted the fact that a large number of IPs makes the analysis hard to manage. In this sense, a 24 IPs were selected to conduct the uncertainty quantification.

The choice of the IPs was made based on the adoption of Source Term related variables as FOMs. Then, they were grouped as follows:

- Core initial inventory.
- Fission product release model (CORSOR-BOOTH).
- Fuel and cladding failure.
- Aerosol characterization.

Considering that the analysis of the accident was focused on the source term, 3 main FOMs have been selected: Iodine, Cesium and Noble gases releases to the environment. FOMs were analysed in relative terms as fraction of the releases from the fuel. Even though the magnitude at the end of the calculation is the main interest, the time history of the “into-environment” fraction released allows paying attention to the release kinetics.

Due to its involvement in the accident evolution, the containment failure time was selected, as Additional Variable (AV) to be studied, as it indicates the onset of the radiological emission to the environment.

The uncertainties have been propagated using Monte-Carlo method and tolerance intervals have been obtained for the main FOMs according to the Wilks’ formula. A sensitivity analysis, based on Pearson’s and Spearman’s Correlation Coefficients (CCs), has also been performed to evaluate the most influential parameters over the main FOMs.

#### 3.1. Uncertainty quantification results.

The main uncertainty analysis was carried out at a specific time (48 h end of the calculation). According to Figure 4, in all realizations, releases begin right after containment failure, and they sharply increase initially, to drastically slow down over time.

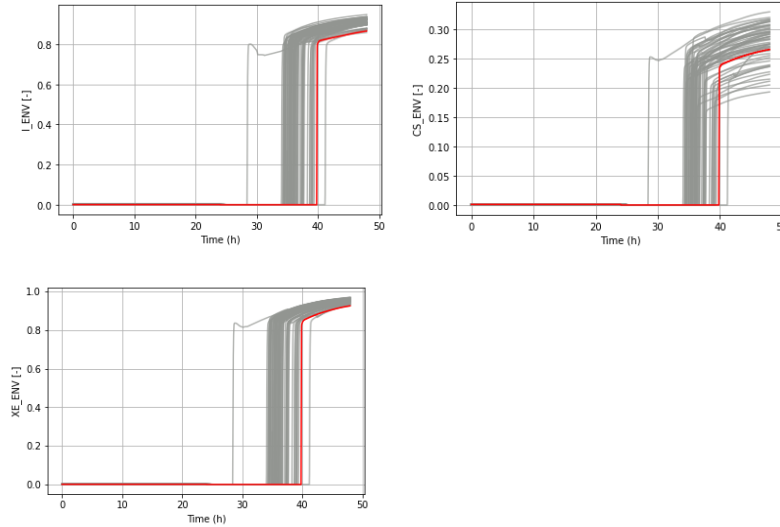


**Figure 4. Dispersion plots**

Evolution in time is similar for all the FOMs: even though the release starts at different times, results seem to converge towards the end of the calculation, where the uncertainty band is quite narrow. The broader band belongs to Cesium and the narrowest one to noble gases. Due to errors in estimation of Cs in the input deck, the UQ observations made with respect to Cs cannot be credited. Here they are kept for the sake of completeness.

Other statistical quantities (such as mean, median, and standard deviation) for the selected FOMs at 48 h are reported in Table 2.

**Table 2. Statistical analysis of the FOMs, at the end of the calculation**

| <b>Statistical parameter</b> | <b>Iodine release to the environment</b> | <b>Cesium release to the environment</b> | <b>Noble gases release to the environment</b> |
|------------------------------|------------------------------------------|------------------------------------------|-----------------------------------------------|
| MELCOR reference case (%)    | 86.57                                    | 26.59                                    | 92.47                                         |
| Mean (%)                     | 90.97                                    | 27.81                                    | 95.25                                         |
| Median (%)                   | 90.995                                   | 28.42                                    | 95.48                                         |
| Lower bound (%)              | 85.88                                    | 19.33                                    | 92.59                                         |
| Upper bound (%)              | 94.71                                    | 33.02                                    | 96.89                                         |
| Standard deviation (%)       | 1.94                                     | 3.22                                     | 1.11                                          |

The scatterplots and the Cumulative Distribution Function (CDF) for FOMs on FPs release are presented in Figure 5 at 48 h. As it can be seen, for all three FOMs, results distribute rather uniformly throughout the FOM space and outliers are not detected.

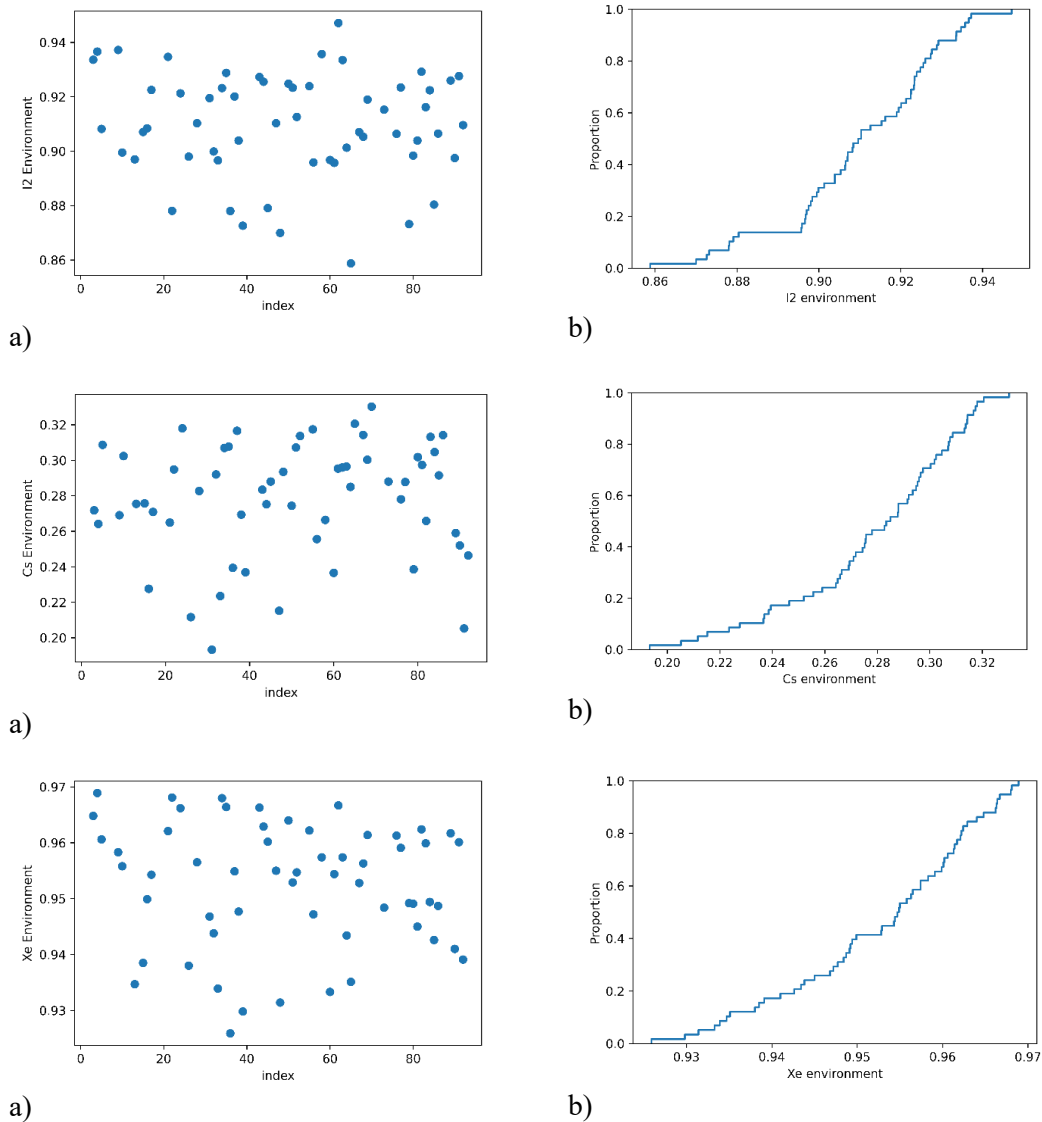


**Figure 5. Scatterplots (a) and CDFs (b) for the selected FOMs**

As expected, noble gases present the highest releases; with values going from 92.5% to 97%, which is consistent with the volatile nature of noble gases. As for iodine, high releases are estimated, just slightly under the noble gases due to its deposition along the transport path between core and environment. Cs counterpart plot is included, although no discussion is given due to the reasons reported in previous paragraphs.

The containment failure time prediction (as AV) was paid attention in the analysis considering the major role of the containment failure on the release of fission products kinetics into the environment. As shown in the Figure 6, the bulk of the realizations estimate that containment failure time lies within 34 h – 40 h. The plot also reveals the presence of a couple of outliers. Two cases show differences with respect to the rest of the calculations:

- In one case, the containment fails slightly later (at around 41 h).

- In the other case, the containment fails much sooner (at around 28 h).

Table 3 summarizes the statistical analysis related to the AV. It can be observed that the standard deviation is small (only 5% with respect to the mean/median value), thus confirming that most data are located within a narrow distance from the mean. The BE prediction is much closer to the upper bound than to the mean/median values.

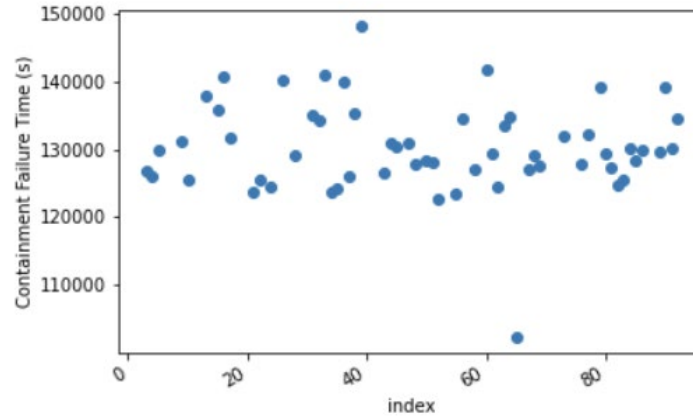


**Figure 6. Scatterplot for the selected AV**

**Table 3. Statistical analysis of the AV**

| Statistical parameter | Time (s) | Time (h) |
|-----------------------|----------|----------|
| MELCOR reference case | 143362.0 | 39.8     |
| Mean                  | 130306.5 | 36.2     |
| Median                | 129564.5 | 36.0     |
| Lower bound           | 102351.0 | 28.43    |
| Upper bound           | 148285.0 | 41.2     |
| Standard deviation    | 6710.7   | 1.86     |

### 3.2. Sensitivity analysis results.

For sensitivity analysis, the Pearson's and Spearman's Correlation Coefficients (CCs) have been considered. As it can be seen in Figure 7 and Figure 8, both coefficients change along the time, according to the progression of the accident. Note that values for both coefficients before the release onset time are meaningless and they are likely associated to negligible releases.

For the present analysis, however, it was decided to focus on one specific time instant, namely 48 h, as in the UA. A number of observations can be done concerning the FOMs:

- **Iodine release.** Both Pearson and Spearman indicate a moderate correlation with the molecular iodine inventory in the gap of rods in the central ring of the core (rinp1\_clad\_I2), which is physically consistent. Other parameters also show a sort of correlation, although notably weaker, like the scale coefficients of Cs in the CORSOR-BOOTH model (C7103\_CS), the particles shape factor for agglomeration (gamma) and the thermal accommodation coefficient (FTHERM).



- Cesium release.** As in the case of iodine, Pearson and Spearman show correlation with the scale coefficients in the release model (C7103\_CS) and the thermal accommodation coefficient of thermophoresis (F THERM). As for the latter, its correlation looks a bit stronger than iodine's, what might make sense because in the case of Cs transport all of it is estimated to be as particles and, hence, subject to the thermal gradients set at different locations of the pathway.
- Xe release.** Unlike the previous two FOMs, sensitivities shown by Pearson and Spearman in the case of Xe release may be seen as misleading and physically hard to support. The only consistency that may be easily understood is the one with Cs scaling coefficients (C7103\_CS). The ones shown with parameters related to particle behaviour, like fslip, stick and ftherm, are just unjustifiable on the basis that Xe is a noble and no relation with aerosols should be expected.

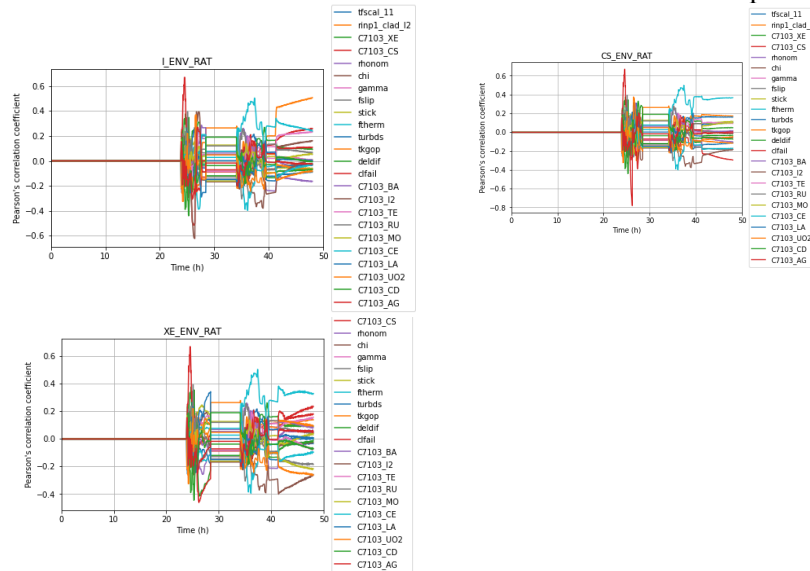


Figure 7. Pearson's coefficients for selected FOMs.

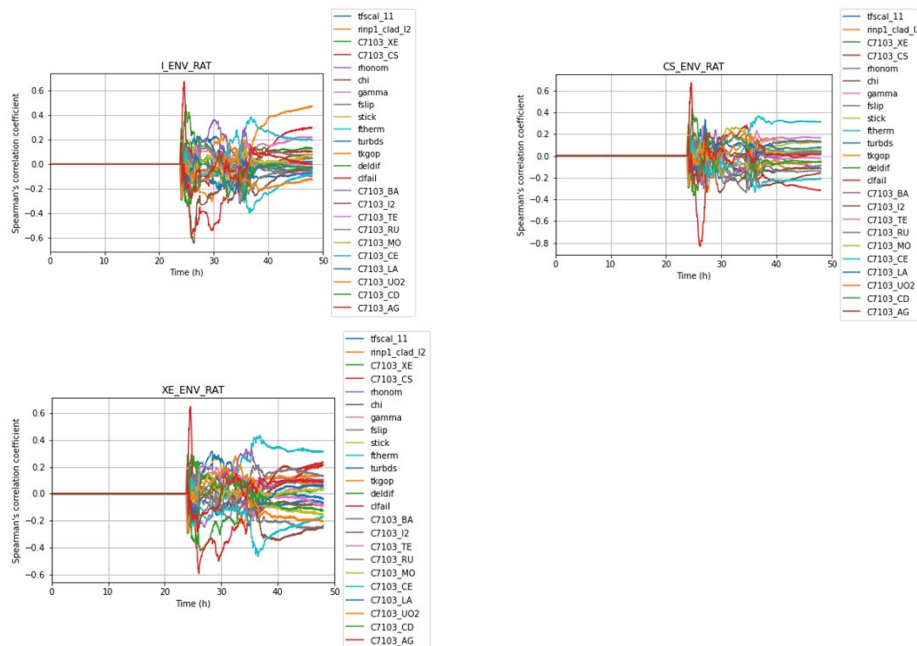


Figure 8. Spearman's coefficients for selected FOMs.

## 4. CONCLUSIONS

The results of the analysis provided some major insights. The ST magnitude is affected by a small uncertainty band. If Iodine is taken as a reference, most of the radiological load initially in the core reaches the environment as a consequence of the early containment failure (at 48 h, release to the environment is higher than 85% of the release from the fuel) and the uncertainty band is just a few percent points. As for the onset time of the release to the environment, it is associated to a significant uncertainty; an approximate five-hour uncertainty band (with an onset time predicted at around 39 h in the base case) might have an effect in the emergency measures to be taken for the Accident Management (AM). Sensitivity analysis did not point at any phenomenon of outstanding significance; however, the time of fuel failure (controlled by a temperature setting) and the diffusional release of radionuclide from fuel have been found to affect the ST to the environment.

## 5. ACKNOWLEDGEMENTS

The authors wish to thank the partners of the MUSA project. This project has received funding from the EURATOM research and training programme under Grant Agreement No -----.



## REFERENCES

- [1] L.L. Humphries, B.A. Beeny, C. Faucett, F. Gelbard, T. Haskin, D.L. Louie, J. Phillips. MELCOR Computer Code Manuals, Vol.1: Primer and User' Guide Version 2.2.14959, SAND2019-12536 O Sandia National Laboratories, October 2019.
- [2] L.L. Humphries, B.A. Beeny, C. Faucett, F. Gelbard, T. Haskin, D.L. Louie, J. Phillips. MELCOR Computer Code Manuals, Vol.2: Reference Manual Version 2.2.14959, SAND2019-12537 O Sandia National Laboratories, October 2019.
- [3] Adams, B.M., Eldred, M.S., Dalbey, K.R., Bohnhoff, W.J., Swiler, L.P., Hough, P.D., Gay, D.M., Eddy, J.P., Haskell, K.H., 2018. DAKOTA : a multilevel parallel object-oriented framework for design optimization, parameter estimation, uncertainty quantification, and sensitivity analysis. Version 5.0, user's manual. <https://doi.org/10.2172/991842>.
- [4] P. Mattie, R. Gauntt, K. Ross, N. Bixler, D. Osborn, C. Sallaberry, and J. Jones., 2016. Uncertainty Analysis of the Unmitigated Long-Term Station Blackout of the Peach Bottom Atomic Power Station (NUREG/CR-7155). U.S.N.R.C.
- [5] Wilks, S.S., 1941. Determination of Sample Sizes for Setting Tolerance Limits. The Annals of Mathematical Statistics 12, 91–96. <https://doi.org/10.1214/aoms/1177731788>.
- [6] M. Angelucci, R. Bocanegra, S. Paci, L.E. Herranz, 2022. Supervised Machine Learning-based Feature Selection in the Frame of BEPU in Severe Accidents. NENE22, Portoroz, Slovenia.